

Linearly Polymerized Benzene Arrays As Intermediates, Tracing Pathways to Carbon Nanotubes

Bo Chen,[†] Roald Hoffmann,^{*,†} N. W. Ashcroft,^{||} John Badding,^{§,⊥,‡} Enshi Xu,^{§,⊥} and Vincent Crespi^{§,⊥,‡,#}

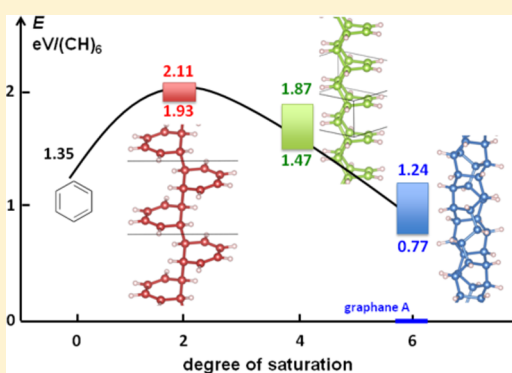
[†]Department of Chemistry and Chemical Biology, Cornell University, Baker Laboratory, Ithaca, New York 14853-1301, United States

^{||}Laboratory of Atomic and Solid State Physics, Cornell University, Ithaca, New York 14850, United States

[§]Department of Physics, [⊥]Materials Research Institute, [‡]Department of Chemistry, and [#]Department of Materials Science and Engineering, Pennsylvania State University, University Park, Pennsylvania 16802, United States

S Supporting Information

ABSTRACT: How might fully saturated benzene polymers of composition $[(\text{CH})_6]_n$ form under high pressure? In the first approach to answering this question, we examine the stepwise increase in saturation of a one-dimensional stack of benzene molecules by enumerating the partially saturated polymer intermediates, subject to constraints of unit cell size and energy. Defining the number of four-coordinate carbon atoms per benzene formula unit as the degree of saturation, a set of isomers for degree-two and degree-four polymers can be generated by either thinking of the propagation of partially saturated building blocks or by considering a sequence of cycloadditions. There is also one 4 + 2 reaction sequence that jumps directly from a benzene stack to a degree-four polymer. The set of degree-two polymers provides several useful signposts toward achieving full saturation: chiral versus achiral building blocks, certain forms of conformational freedom, and also dead ends to further saturation. These insights allow us to generate a larger set of degree-four polymers and enumerate the many pathways that lead from benzene stacks to completely saturated carbon nanotubes.



INTRODUCTION

Experimental studies of benzene compression date back a century.¹ As the pressure is increased, the molecular solid undergoes several structural phase transitions and then transforms into amorphous products, at a relatively low pressure.^{2–7} Recently, Fitzgibbons et al.⁸ have for the first time recovered ordered products in slow decompression of benzene from 20 GPa. The partially crystalline product comprises one-dimensional (1-D) sp^3 C–H nanotubes whose diameter is approximately 6.4 Å, the reported distance between packed threads.⁸

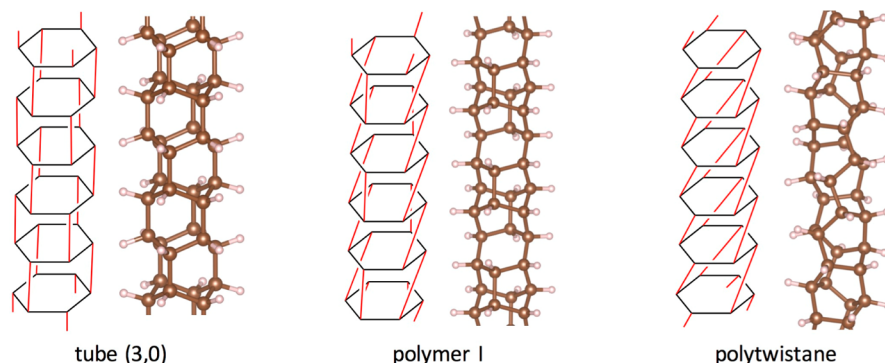
Before this experimental finding, at least three groups, each from a very different perspective, predicted three structures of thin 1-D thread-like sp^3 C–H polymers (Scheme 1). The three structures were given distinct names: tube (3,0),⁹ polymer I,¹⁰ and polytwistane.^{11,12} Tube (3,0) was generated by the Crespi group by thinking about saturating all the sp^2 carbons in a (3,0) carbon nanotube with outward-pointing hydrogen atoms.⁹ The Cornell group found that benzene phase-V at about 80 GPa spontaneously collapses upon relaxation into a 1-D polymer which they called polymer I.¹⁰ The Trauner group constructed the polytwistane structure by contiguous linear extension of twistane with ethano bridges;^{11,12} they also synthesized oligomeric approaches to the polymer.¹¹ Although the three structures look rather different, they all can be viewed as a linearly polymerized stack of $(\text{CH})_6$ rings, only differing in

inter-ring connection patterns. Other $(\text{CH})_n$ structures have been suggested, but of higher dimensionality. They include 2-D graphanes^{13,14} and 3-D arrays.^{15–18}

What is the structure of the nanotubes that were synthesized experimentally, and what alternatives are theoretically possible for ordered completely saturated benzene polymers? In the original publication, Fitzgibbons et al.⁸ proposed a random polymer intermediate in structure between tube (3,0) and polymer I as an approximant to the nanotube. The resulting calculated pair distribution functions match the experimental data better than either tube (3,0) or polymer I alone. On the other hand, Maryasin et al.¹⁹ suggested that polytwistane might be a component of the synthesized nanotubes by comparing the calculated NMR spectrum of polytwistane to the experimental data. Very recently, Xu, Lammert, and Crespi²⁰ have systematically enumerated sp^3 C–H nanotubes built from a stack of benzene molecules, finding at least 50 distinct stable structures with small unit cells, excluding structures in which the former benzene rings are connected by one bond. The most stable 15 of these are within 0.48 eV/ $(\text{CH})_6$ of each other and include tube (3,0), polymer I and polytwistane.

Received: August 26, 2015

Published: October 21, 2015

Scheme 1. Three Predicted Structures of 1-D sp^3 C–H Nanothreads, Showing Both Schematic and Relaxed Structural Models

In this and subsequent papers, we will detail three distinct theoretical approaches to elucidating the mechanism of formation of a completely saturated carbon nanothread from benzene: (1) an enumeration of partially saturated $(CH)_6$ stacks that might arise from benzene and an examination of plausible pathways connecting benzene, partially, and fully saturated $(CH)_6$ stacks; (2) the use of a helium compression chamber to emulate what happens to benzene under pressure;²¹ and (3) an examination in detail of the primary initiation and propagation steps in the pressure-initiated polymerization of benzene. In this paper we discuss briefly two plausible mechanisms of nanothread formation based on the solid-state structure of benzene phase III and go on to a reasonably complete (for small repeat units) enumeration of possible intermediate polymers, following the first approach. That enumeration makes no presumption of the mechanism of formation of the linear polymers obtained. Investigations using the second and third approaches are ongoing and will be reported in due course.

RESULTS AND DISCUSSION

The Solid Benzene Structure. We begin with the structure of solid benzene. Two phase diagrams of benzene have been proposed previously, one by Thiéry and Léger²² and the other by Ciabini et al.^{6,7} In Thiéry and Léger's notation, the most relevant phase is benzene phase III, in space group $P2_1/c$. This is stable from about 4 GPa up to 20–25 GPa,^{23,24} which covers most of the pressure range at which the synthesis of nanothreads was conducted. The structure of benzene phase III ($P2_1/c$) was optimized by us at 20 GPa, in a manner described in the Theoretical Methods section. Figure 1 shows a 3D-printed model of the structure,²⁵ and Figure 2 shows three perspective views along the crystallographic axes.

The volume compression of this structure relative to 1 atm is calculated to be 1.59. The compression is accomplished, as

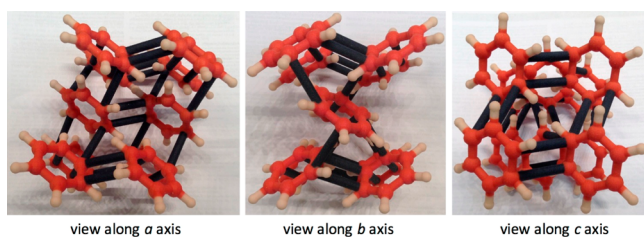


Figure 1. 3D printed model of the optimized structure of benzene phase III ($P2_1/c$) at 20 GPa.

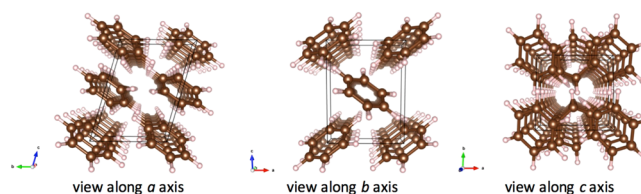


Figure 2. Perspective views of benzene phase III ($P2_1/c$) structures at 20 GPa, along the three crystallographic axes.

expected, by reducing the space between molecules, without materially affecting the geometry of the molecule. The closest nonbonded $H\cdots H$ contact falls from 2.36 Å at 1 atm to 1.71 Å at 20 GPa, but the benzene C–H and C–C bonded distances over the same pressure interval change only from 1.09 to 1.08 Å and 1.40 to 1.38 Å, respectively.

Along either the a or b direction of this crystal structure, one observes benzene stacks. The benzene molecules are in planes parallel to each other, but the planes are not perpendicular to the stack axis. In other words, the stacks are composed of “slipped” benzene rings. The view of the b stack in Figure 3 (left) shows this clearly. Returning to Figures 1 and 2, along the c direction no obvious stacks can be seen.

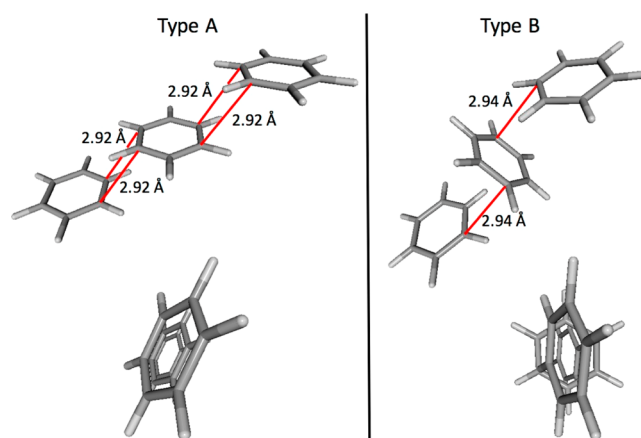
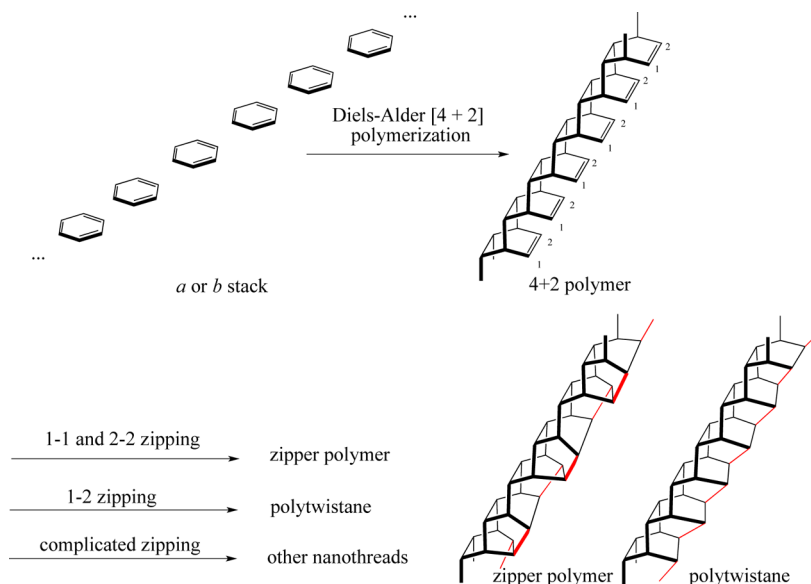


Figure 3. Two types of short $C\cdots C$ contacts in benzene phase III.

One Polymerization Sequence Starting with Diels–Alder Reactions. C–C bond formation between benzene molecules is a reasonable initiating step for the polymerization,²⁶ so we examined the theoretical benzene phase III structure at 20 GPa to identify short $C\cdots C$ contacts. Similar to what Ciabini et al.⁷ found and called the nearest-neighbor C–C

Scheme 2. Proposed Mechanism for the Formation of Nanothreads by Fitzgibbons et al. and Olbrich et al

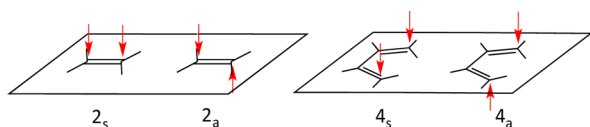


distance, there are two types of such contacts in the benzene phase III structure, as shown in Figure 3. In type A, the adjacent benzene molecules are both in the same *b* stack, and there are two equidistant C...C contacts at distance of 2.92 Å. In the calculated structure of graphite at 20 GPa, the interlayer distance is about the same, down from 3.35 Å at $P = 1$ atm.

The pair of equidistant short C...C contacts between two benzene molecules in stack *b* (and similarly in stack *a*) points to the possibility of forming two C–C bonds at the same time. However, this is unlikely, because such a process is a locally symmetry-forbidden $[2_s + 2_s]$ cycloaddition,²⁷ which usually has a very large activation barrier. Furthermore, the process would form diradicals and four-membered rings along the chain. In the study of the completely saturated nanothreads, there is one structure with cyclobutane entities in the 15 lowest-energy threads, and all other structures with four-membered rings are 0.47–1.64 eV/(CH)₆ above the lowest-energy structure.²⁰ There is some evidence for a small measure of cyclobutane substructures in the nanothreads.⁸ Overall, we judge the four-membered rings to be destabilizing and do not consider structures containing them in the enumeration below. Instead of the symmetry-forbidden $[2_s + 2_s]$ cycloaddition, a symmetry-allowed $[4_s + 2_s]$ cycloaddition is more plausible (Scheme 2), as in the mechanism proposed by Fitzgibbons et al.⁸ and Olbrich et al.²⁸

The nomenclature of n_s , n_a addition for olefins comes from the concepts of orbital symmetry control, the Woodward–Hoffmann rules.²⁷ In these, one speaks of addition to an ethylene (a two-electron component) or butadiene (four-electron) or an n π -electron polyene in general, as proceeding on the same (*supra*, subscript *s*) or opposite (*antara*, subscript *a*) faces of the unsaturated molecules (Scheme 3).

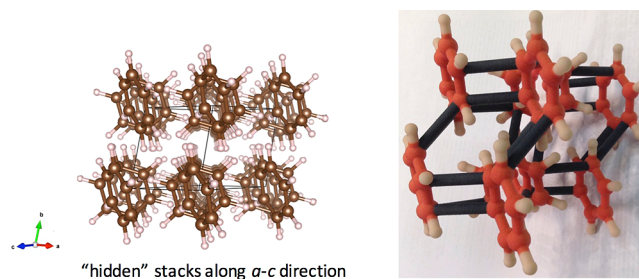
Scheme 3. Modes of Additions to Ethylene and Butadiene That Are Discussed in This Paper



To achieve the proper geometry for $[4_s + 2_s]$ cycloadditions, all benzene molecules need to slide/slip substantially. In the tightly packed solid-state crystal at pressure, this motion could also have a large barrier. We call a sequence of these $[4_s + 2_s]$ cycloadditions the “4 + 2 polymerization” and the polymer that results the “4 + 2 polymer”.²⁹ In time we will see its optimal structure.

The 4 + 2 polymer can in principle undergo further transformations: double-bond “zipping” to produce nanothreads. Depending on how the zipping occurs, different nanothreads can be formed: the zipper polymer⁸ and polytwistane²⁸ of Scheme 2 can both be formed from the same 4 + 2 polymer. More heterogeneous zipping could lead to still other nanothreads.

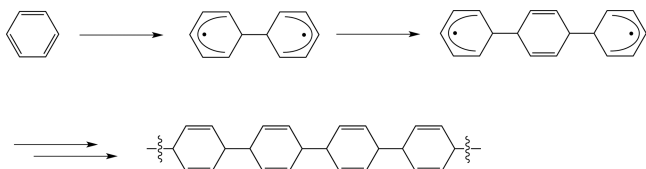
Another Mechanism Starting with *para* Polymerization. Stacks are in the eyes of the beholder, and in the benzene III structure at 20 GPa there is a second ring contact (and a stack featuring it) close to the 2.92 Å of type A. This is type B of Figure 3; in it, the molecules constituting the stack lie along the *a*–*c* direction (the diagonal direction in Figure 2b) in benzene phase III. Figure 4 reveals these “hidden” stacks. The molecules forming them are certainly not parallel, but there is one short C...C contact between them, at a distance of 2.94 Å. Actually, for each benzene molecule there are two such short C...C contacts, one going “up”, the other going “down” the stack; the two short contacts are at opposite positions (*para*)

Figure 4. “Hidden” stacks of benzene in the structure of benzene phase III ($P2_1/c$) at 20 GPa.

on the benzene ring. This feature leads us to think of another polymerization mechanism.

Suppose nucleation leads to the formation of one C–C bond between the two short-contact carbon atoms of adjacent benzene molecules in the *a*–*c* stack. As shown in Scheme 4, a

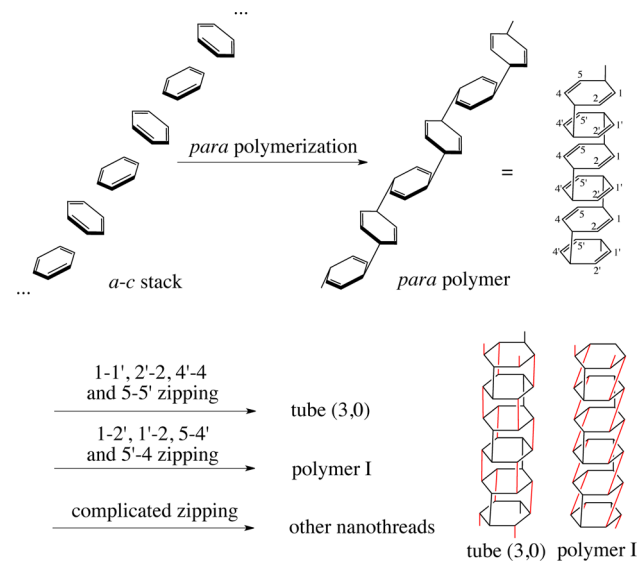
Scheme 4. Schematic Drawing of Initiation and Propagation in Hypothetical *para* Polymerization Mechanism along the *a*–*c* Stack



reactive diradical will be formed, the initiator of a polymerization. If this diradical were to react further with a third benzene molecule along the *a*–*c* stack, given the distribution of unpaired electrons in the diradical, a second bond will be formed, at the *ortho* and *para* positions of each ring. The *ortho* positions appear distant from other benzenes, so the newly formed bond is expected to be *para* to the previously formed one, which is, as we mentioned, a relatively short contact to other benzenes in the crystal. If this kind of reaction goes on, one ends up with a polymer of units of 1,4-cyclohexadiene. We tentatively term this process “*para* polymerization”, and the polymer formed the *para* polymer.

This process leads to another mechanism of nanothread formation (Scheme 5). In the *para* polymer (if we ignore for a

Scheme 5. Another Mechanism for Nanothread Formation, Now Along the *a*–*c* Direction in Benzene Phase III Structure



moment the conformational relationship between adjacent rings and place all six-membered rings in an eclipsed conformation), double-bond “zipping” in both sets of double bonds could lead to a variety of nanothreads, as shown in Scheme 5.

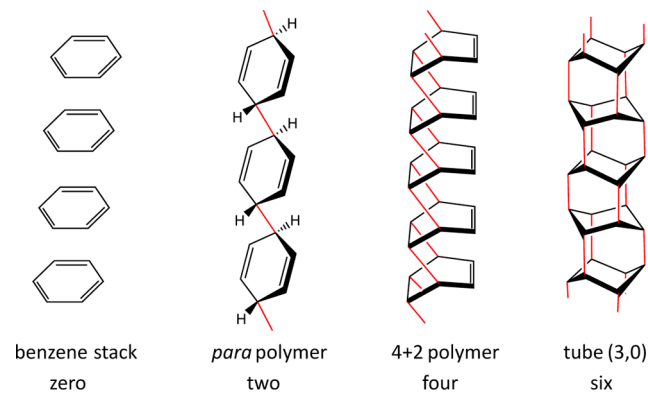
We note here that the Bini group has suggested zwitterionic intermediates in the initiation step⁷ or the possible involvement of an excited state of benzene.²⁶ The detailed

mechanism of nucleation (initial bond formation) and propagation will be discussed by us in a subsequent contribution.

Degree of Saturation. Are there other mechanisms of nanothread formation beyond those outlined in Schemes 2 and 5? Perhaps the structures of partially saturated benzene polymer intermediates could suggest such mechanisms to us. So we proceed to enumerate all such intermediates, or at least as many simple ones (we will make “simple” more precise below) as there can be. We should make it clear that while we use the terminology of cycloadditions to discuss the formation and transformations of the polymers, that this is just a way of delineating the isomeric potentialities that result from such cycloadditions. How the reactions are nucleated and might actually proceed is not discussed in this paper; we assure the reader that we will return to these questions in subsequent work.

We begin by defining the “degree of saturation”, to categorize these polymers and differentiate them from the two end points, i.e., molecular benzene and fully sp^3 -bonded nanothreads. The degree of saturation varies from 0 to 6; it counts how many sp^3 carbons reside in each $(CH)_6$ ring. A stack of benzene molecules (shown in Scheme 6) has degree of saturation zero.

Scheme 6. Degree of Saturation Evolving from 0 to 6

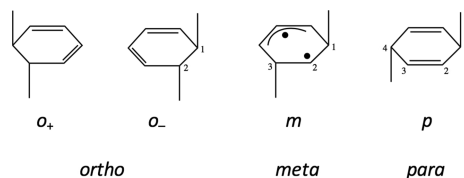


The *para* polymer of Scheme 5 has degree of saturation two, and the 4 + 2 polymer of Scheme 2 has degree of saturation four. Any fully saturated nanothreads, such as tube (3,0), has degree of saturation six. Structures with odd degrees of saturation would be polyradicals; they might be reaction intermediates, but bonds would likely form between radical centers to reach the next highest even degree of saturation. Therefore, we did not consider these structures in the following enumeration.

Enumeration of Degree-Two Polymers. We start with an accounting of degree-two polymers. There are many ways to accomplish such an enumeration; we used one method that we thought straightforward, constructing the polymer structures from building blocks and focusing on the newly saturated centers.

Possible building blocks for a degree-two polymer are shown in Scheme 7. Depending on the relative positions of the two sp^3 carbons in the ring, we can label each building block *o*, *m*, or *p* (short for *ortho*, *meta*, or *para*). Note that the two sp^3 carbons in each ring must bond in different directions, one “up” and the other “down” the stack. Otherwise we do not obtain a polymer, just a dimer.

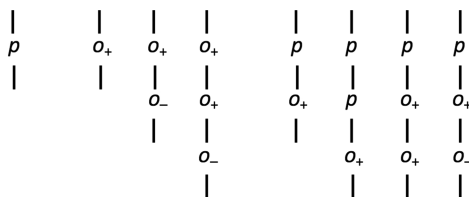
Scheme 7. Building Blocks for Degree-Two Polymers



The *meta* building block is a diradical; for reasons mentioned above, we do not consider these structures in the enumeration. The *ortho* building block is clearly chiral. The two mirror images of that block can yield distinct structures in certain circumstances, as we will see. For this reason, we differentiate them explicitly in the enumeration with different labels, o_+ and o_- (o stands for *ortho*, subscripts $+$ and $-$ for non-superimposable mirror images).

By connecting and propagating the o_+ , o_- , and p building blocks in different sequences, one can form different polymers. There is an infinity of such sequences, and we limit ourselves to $Z < 4$, i.e., a maximum of three building blocks per crystallographic unit cell. Scheme 8 shows the set we studied.

Scheme 8. Sequences of Building Blocks for Degree-Two Polymers That Have Been Considered in the Enumeration



The sequences in Scheme 8 are grouped into three classes: *para* building block alone, *ortho* alone, and mixed *para* and *ortho*. Due to the chirality of the *ortho* building block, whenever there are two *ortho* building blocks in the repeat unit stereoisomers appear, for example, $-p-o_+-o_+$ versus $-p-o_+-o_-$. These will be distinct, isomeric polymers, not interconvertible without C–C bond breaking and reforming. Certain symmetries limit the number of distinct degree-two intermediates. For example, the $-o_+-o_-o_+$ repeat unit represents the same sequence as $-o_+-o_+-o_-$. The problem resembles that of enumerating the enantiomeric possibilities in a stereoregular polymer with chiral monomer building blocks.³⁰

We now build realistic models for these sequences. In each case we used GaussView³¹ to construct an oligomer, terminated with hydrogens, of a certain sequence; the geometry of the oligomer was coarsely optimized by the “Cleaning Structures” function of GaussView. We then used Molden³² to cut out a unit cell from the central part of the oligomer, generating from it a polymer with periodically repeating units. The resulting model polymer was then optimized at the density functional theory level in VASP,³³ spacing the polymer threads far apart from their replicas in a tetragonal cell.

Figure 5 shows the optimized structures of polymers built solely from the *para* building block. These polymers differ in the numbers of $(\text{CH})_6$ units in the repeating cell. There are two $Z = 3$ polymers; to build these we were guided by some considerations (described in Figure S1 in the Supporting Information (SI)) of conformational preferences of diradical intermediates. These four structures are all local energy minima with energies 0.63 to 0.72 eV/ $(\text{CH})_6$ higher than benzene. These four polymers are not distinct isomers; they are conformers that are interconvertible through rotations around C–C bonds. We have not yet studied the barrier to conformer interconversion, which might not be as easy in a pressurized solid.

Following the construction principle of Scheme 8, we go on to build other degree-two polymers. Figure 6 shows the optimized structures of seven of these (not counting enantiomers), each with a distinct bonding topology. Only the lowest-energy conformers are shown for each isomer. For structures of all conformers, see Figure S2 in the SI.

The energies of these structure are very close, all within 0.14 eV/ $(\text{CH})_6$. This is easy to understand. The *ortho* and *para* units can be modeled by 1,3- and 1,4-cyclohexadiene molecules. Our molecular calculations show that the energy difference between these two molecules is <0.01 eV/ $(\text{CH})_6$, in agreement with the experimental data from NIST Chemistry Webbook.³⁴ In addition, our calculations on benzene dimers with only one inter-ring C–C bond (i.e., diradicals) show that the energy difference between conformers is ~ 0.05 eV/ $(\text{CH})_6$. These small energy differences between the *ortho* and *para* building blocks and between conformers yield the small energy differences between different degree-two polymers.

Collapse of Degree-Two Polymers to Degree-Four Polymers. One interesting finding from the enumeration of degree-two polymers is that some conformations of these, upon optimization, collapse without barrier to degree-four polymers. We found six such transformations, two of which are shown in

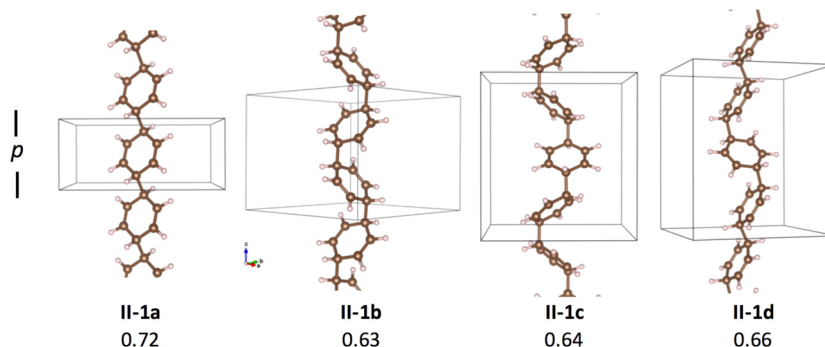


Figure 5. Optimized structures of degree-two polymers built solely from the *para* building block. In the structure number, the Roman II gives the degree of saturation; the Arabic numeral numbers topologically distinct structure; and the letter labels different conformers. Number at the bottom of each structure gives its energy relative to benzene in units of eV/ $(\text{CH})_6$.

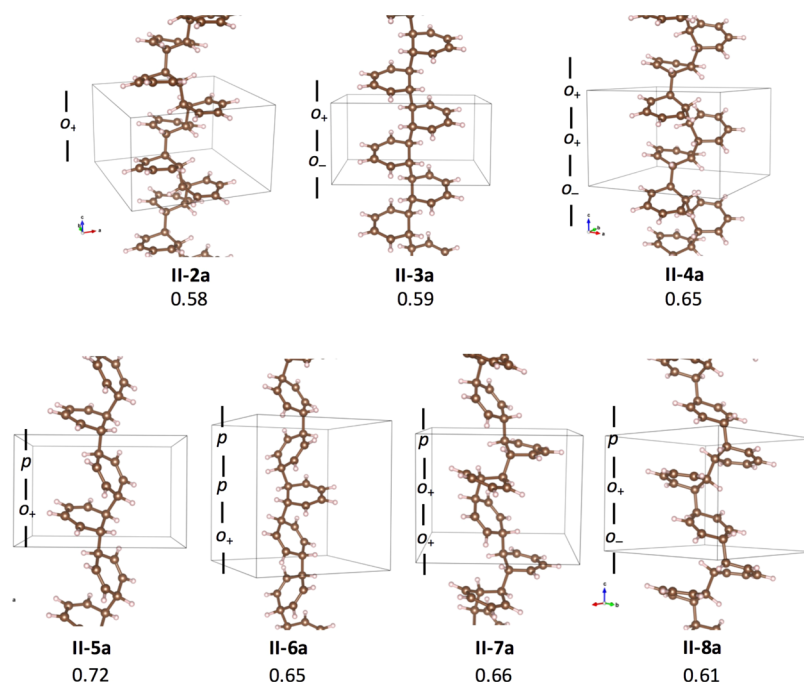


Figure 6. Optimized structures of lowest-energy conformers of other topologically distinct degree-two polymers. In the structure number, the Roman II gives the degree of saturation; the Arabic numeral numbers serially topologically distinct structure; and the letter labels different conformers (higher energy conformers are shown in SI). The number at bottom of each structure shows its energy relative to benzene in units of $\text{eV}/(\text{CH})_6$.

Figure 7; the rest are given in Figure S3 in the SI. We came on these by exploration of conformational changes in the parent polymers of Figure 6.

In each case, the reason for the high energy of the unstable conformations is the repulsion between $\text{C}=\text{C}$ double bonds in adjacent rings, in turn a consequence of fairly short inter-ring distances. For example, in the unstable conformer II-2b of the $-o_+-$ polymer the shortest such $\text{C}\cdots\text{C}$ distances are 2.40 Å

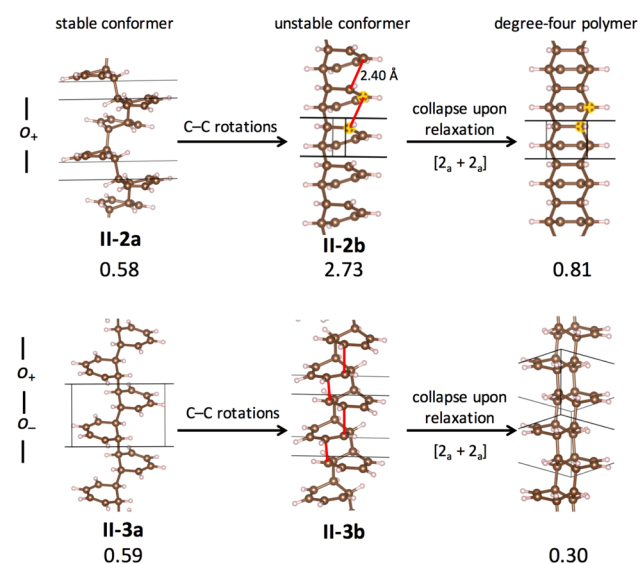


Figure 7. Two examples of an unstable conformer of a degree-two polymer collapsing upon relaxation to a degree-four polymer. Both transformations feature $[2_a + 2_a]$ cycloadditions along the polymer axis. The numbers below each polymer show its energy relative to benzene, in unit of $\text{eV}/(\text{CH})_6$.

(Figure 7), which is slightly longer than the $\text{C}\cdots\text{C}$ distances in transition-state structures of typical cycloadditions.^{35,36} This unstable conformer is not an energy minimum, and its single-point energy is very high, 2.15 $\text{eV}/(\text{CH})_6$ above the most stable conformer II-2a. Upon relaxation, it collapses without barrier to a degree-four polymer, in this case, the $4 + 2$ polymer, by a sequence of $[2_a + 2_a]$ cycloadditions. As we will see in a later section, other kinds of cycloaddition that take a degree-two polymer to a degree-four polymer involve $[4_a + 2_a]$, $[4_a + 4_a]$, and $[4_s + 4_s]$ cycloadditions.

Note that although a simple $[2_a + 2_a]$ or $[4_a + 4_a]$ cycloaddition of two benzenes is symmetry forbidden, the reactions at hand are not two-component cycloadditions, but (in principle) infinite polymerizations. We do not think the orbital symmetry constraints apply; there are other impediments to the reactions that will be discussed later.

These spontaneous collapses upon relaxation, such as the two shown in Figure 7, are enlightening in the sense that they suggest possible reaction pathways leading from degree-two polymers to greater saturation and ultimately fully saturated nanotreads. We will examine these pathways in detail in the last section.

Enumeration of Degree-Four Polymers. The same building-block strategy was used to enumerate degree-four polymers. However, we note that there is another means to achieve this end: based on the work of enumeration of degree-six nanotreads by some of us,²⁰ degree-four polymers could be obtained by “going back” from degree-six nanotreads, breaking just two bonds per each $(\text{CH})_6$ ring in those threads. The results of the second strategy are given in Figure S4 in the SI. It turns out that fewer degree-four polymers are found by the second strategy than the first. This is because all the degree-four polymers found by the second strategy must be by definition “productive” in leading to degree-six nanotreads. However,

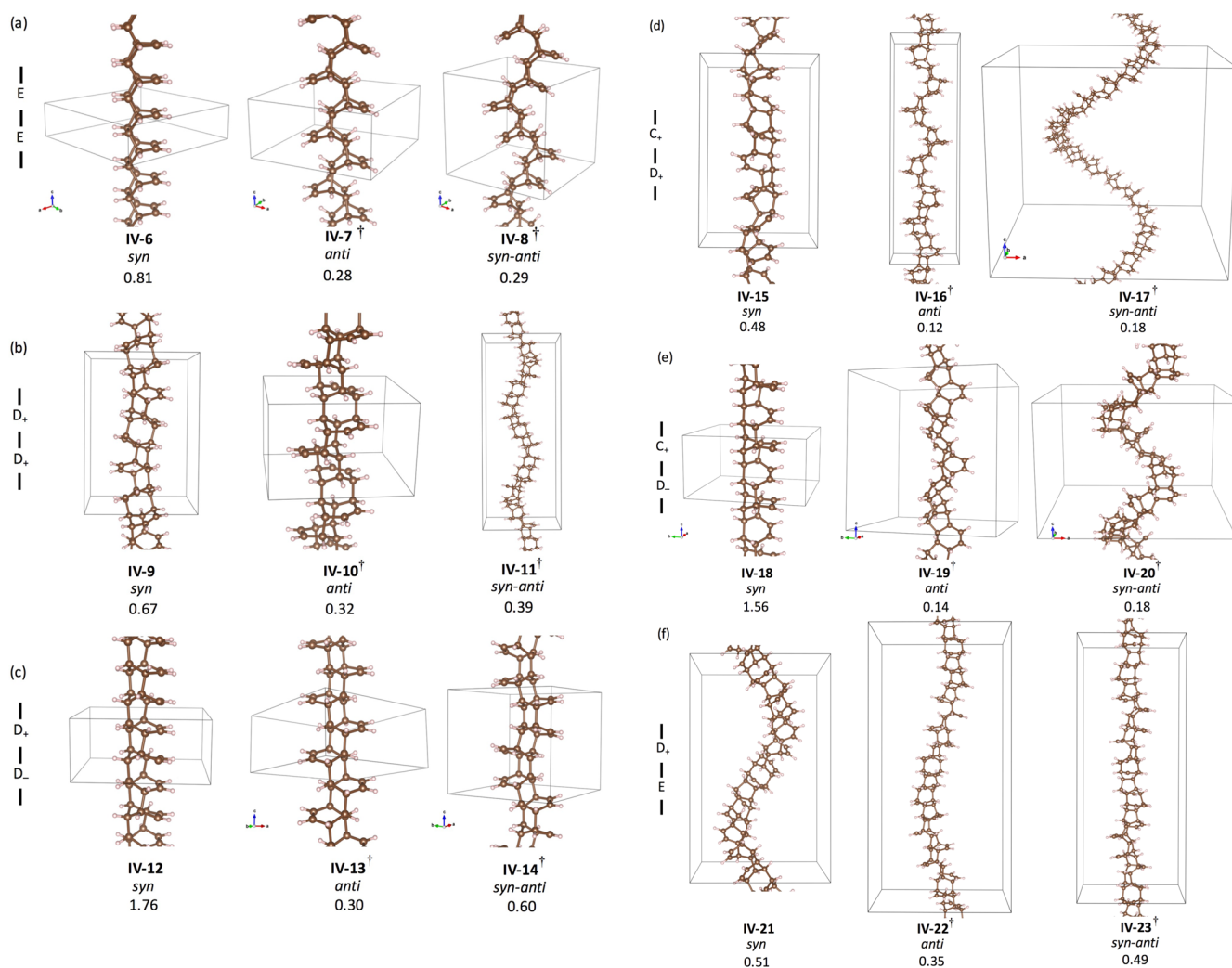
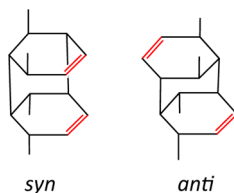


Figure 9. Optimized structures of topologically distinct degree-four polymers built from $2u2d$ units. In the structure number, the Roman IV gives the degree of saturation, and the Arabic numeral numbers serially topologically distinct structure. The symbol † indicates this structure is a dead end toward further transformation to a degree-six nanothread. Numbers at bottom of each structure show its energy relative to benzene in unit of eV/(CH)₆. Three isomers (*syn*, *anti*, and *syn-anti*) of the (a) $-E-E-$, (b) $-D_+-D_+-$, and (c) $-D_+-D_--$ sequences. (d-f) Three isomers of the $-C_+-D_+-$, $-C_+-D_--$ and $-D_+-E-$ sequences.

Scheme 11. The *syn/anti* Configurations for Degree-Four Polymers



isomer IV-6 is what we called 4 + 2 polymer in Scheme 2. It should be noted that several oligomers of IV-6 have been synthesized; the longest contains six benzene units and chlorine substituents. It adopts a curved or bowed structure due to double-bond repulsion.²⁹ That bowing is reproduced in calculations we did on oligomers. The natural tendency to curve leads to a high energy when that deformation is not allowed to occur, as in our calculation for polymer IV-6 in a geometry with a unit cell containing only one (CH)₆ ring. We cannot calculate the large unit cells that bowing brings about. But if a unit cell with two (CH)₆ rings is used, the structure

collapses upon relaxation to a degree-six nanothreads, the zipper polymer in Scheme 2.

Similar to the situation with the $-E-E-$ polymer, three *syn*, *anti*, and *syn-anti* isomers can also be built for other $2u2d$ sequences. If larger topological cells were studied, we would of course find more such isomers. These structures are shown in Figure 9b-f. One notices that *syn* isomers are always higher in energy than others, due to repulsion between double bonds at shorter distances.

Unlike the case of degree-two polymers (but analogous to degree-six nanothreads), some isomers of degree-four polymers are helical. To construct and optimize the structures of these helical polymers, we deviated slightly from the method used for degree-two polymers. After construction and coarse optimization of the oligomer structure of a certain polymer with GaussView,³¹ we reoptimized its structure using either the semiempirical PM3³⁸ method or the DFT B3LYP³⁹ method with Gaussian09.⁴⁰ Then we cut out a unit cell from the oligomer with Molden³² for further VASP³³ optimization.

Note that the PM3 or B3LYP optimized structures of some helical oligomers have an apparently irrational helical pitch, i.e.,

they do not repeat themselves after a multiple of 2π . In those cases, we use a periodic approximant, i.e., we force the helices to repeat after either a 2π or 4π cycle, at whichever point the helix is closest to repeating itself. The strain introduced by this deformation is modest, without significant changes in bond length or angle, so we think that the energies of these periodic approximants will not differ much from the energies of the ideal aperiodic helices.

As shown in Figure 9, the helical polymers can have very large crystallographic unit cells, although topologically they are made up of at most two units. Their energies are quite low, <0.51 eV/(CH)₆ higher than benzene, and lower than those of degree-two polymers.

Collapse of Degree-Four Polymers to Degree-Six Nanotreads. Just as we observed computationally the collapse of some degree-two polymers to degree-four, we might expect that some degree-four polymers collapse upon optimization to degree-six nanotreads. Collapse should occur in degree-four polymers in which double bonds are close to each other, such as the *syn* isomers in Figure 9. It appears that this is less common for degree four polymers; we did not observe any spontaneous, barrier-less collapse for any *syn* isomers shown in Figure 9, nor for any polymers in Figure 8, although in some of these double bonds are indeed close to each other. We did observe, however, as we mentioned, the spontaneous collapse of IV-6 with two molecules per unit cell to a nanotread. The message is clear: as we consider mechanisms in our next papers, we have to look at larger unit cells.

It is also clear that some of the degree-four threads are dead ends (marked by a † in the figures, i.e., they cannot continue to degree-six because the double bonds in some adjacent rings are far away from each other, such as the *anti* and *syn-anti* isomers in Figure 9.⁴¹

Relative Energies of (CH)_n Species. All the polymers studied, whatever their degree of saturation, have the same formula, (CH)_n. A certain perspective on the polymerization is gained by putting their energies on a single diagram. Previous calculations used a variety of methodologies, so we repeated some of the calculations with the same method: VASP calculations for either molecules or extended systems. Benzene, its molecular dimers, and graphanes are now included in Figure 10. Note that due to the inclusion of a dispersion correction in the present calculations, the computed energy difference between benzene and graphane A is 0.45 eV/(CH)₆ larger,¹⁴ and the energy differences between nanotreads and graphane A are 0.20 eV/(CH)₆ larger²⁰ than those obtained from our previous calculations.

Graphane A,¹⁴ with all chair six-membered rings, is the lowest-energy (CH)_n species and is set as energy reference. The other graphane isomers are slightly higher in energy and are not shown in Figure 10. With the same degree of saturation six as graphane, the 15 lowest-energy nanotreads contain four, five, six, seven-membered and even larger rings, and these rings are not necessarily in their optimal conformations (for example, the “chair” conformation for six-membered rings) due to the constraints of forming a 1-D polymer. So nanotreads are naturally higher in energy than graphane A.

There is an obvious trend of energy descending with degree of saturation from 2 to 6. The conversion of sp² C=C double bonds into sp³ C–C single bonds is exothermic, because a σ bond is stronger than a π bond. The exothermicity can be roughly estimated from the difference in bond energy between

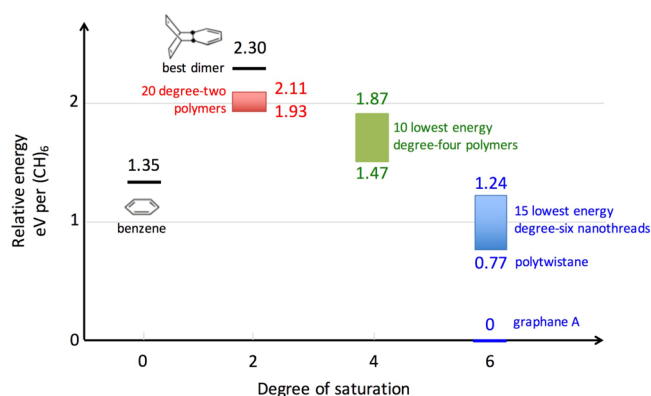


Figure 10. Energy diagram of (CH)_n species in vacuum. Black indicates molecules and colors extended systems, using different colors for different degrees of saturation. The same theoretical methods were used for calculating all these species, either molecules or extended systems. Energies in this diagram are relative to the lowest-energy graphane, not benzene as in previous figures, in units of eV/(CH)₆.

one double bond and two single bonds,⁴² C=C → 2 C–C, ΔH per double bond = $146 - 2 * 83 = -20$ kcal/mol (-0.9 eV). Alternatively one could look at one-third of the experimental heat of the reaction for three ethylenes → cyclohexane,⁴³ in which three π bonds are converted into three σ bonds: ΔH per double bond = -22.3 kcal/mol (-1.0 eV).

Thus, polymers with degree-six saturation are expected to be more stable than degree-four species, which should be more stable than degree-two systems. This expectation is true for many, but not quite all cases. Some particularly unfavorable degree-four polymers are higher in energy than degree-two polymers, and some degree-six nanotreads are higher in energy than degree-four polymers due to unfavorable conformations or ring structures. To clearly show the overall trend, we only give energies of the 10 lowest degree-four and the 15 lowest degree-six polymers in Figure 10.

Not unexpectedly, benzene, with degree of saturation zero, does not follow the trend. Its energy is lower than all degree-four polymers and slightly higher than the 15 lowest degree-six nanotreads. Benzene is aromatic; it acquires additional stabilization by delocalizing its 6 π electrons.⁴⁴

Plausible Reaction Pathways from Benzene Stacks to Degree-Six Nanotreads. With the structures of degree-two, four, and six polymers in hand, we next examined plausible pathways that could take benzene to polymers of higher degrees of saturation. In these examinations, we only considered $Z_{\text{topo}} < 3$ for all polymers.

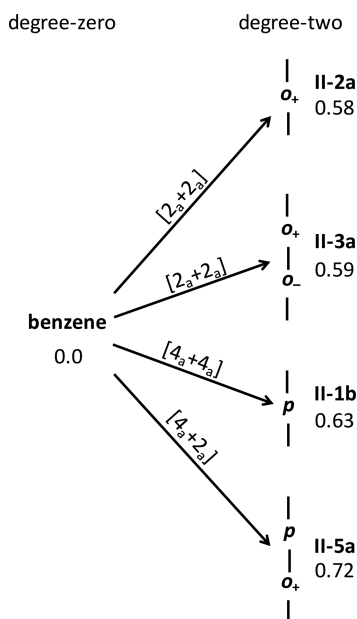
We start with transformations from a benzene stack to a degree-two polymer. A relationship is needed between three concepts that have entered our discussion: (a) the cycloaddition reaction stereochemistries present from the early days of orbital symmetry control (Scheme 3); (b) the chiral and achiral building blocks we found useful in enumerating the degree-two and four polymers (Schemes 7 and 9); and (c) the intuitively formed zipping reactions of Schemes 2 and 5.

We must mention here again that the cycloaddition terminology at this point carries no implication as to whether the reaction will be facile or difficult. The normal rules of orbital-symmetry control do not apply to the infinite sequence of cycloadditions involved. Nor do we know, or mean to imply, that the reactions forming these polymers are concerted single-crystal to single-crystal transformations; they are very likely

nucleated and stepwise with nucleation occurring singly or at random in the crystal. What really happens is material for future work; we just do not know in atomistic detail what happens. We use the cycloaddition terms because they are eminently descriptive of how the resulting connectivity is established.

In going from benzene to degree-two polymers, one double bond in each ring gets saturated; two bonds form for each ring, one going “up” and the other going “down” the stack. As shown in Scheme 12, there are three types of cycloadditions that are productive toward degree-two polymers, $[2_a + 2_a]$ (leading to $-o_+ -$ and $-o_+ - o_- -$), $[4_a + 2_a]$ (to $-p - o_+ -$), and $[4_a + 4_a]$ (to $-p -$).

Scheme 12. Plausible Pathways from Benzene to Degree-Two Polymers^a

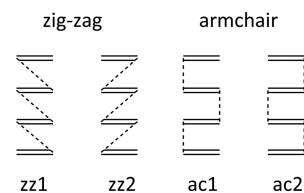


^aThe name and energy, in units of eV/(CH)₆, of each polymer are given next to the sequence.

The reader will notice that the transformations shown in Scheme 12 go to only four of the eight degree-two polymers we discussed earlier. The reason for this limitation is two-fold: first, as we will soon see, one can generate all the 23 degree-four polymers from these four; second, like it or not, we have to apply a constraint on Z_{topo} in isomer enumeration. So the degree-six nanothreads previously enumerated have a $Z_{\text{topo}} \leq 2$, and so do the degree-four polymers just enumerated by us. The other four degree-two polymers, the ones not shown in Scheme 12, would lead to some (many) higher Z_{topo} degree-four and degree-six polymers. So we leave them out.

We also have the relationship between addition stereochemistry and chiral or achiral saturated unit formation. The zipping motions on from the degree-two polymers, which were so easy and natural to draw (Schemes 2 and 5), are obviously $[2_a + 2_a]$ cycloadditions. But in fact they are stereochemically complicated, when occurring sequentially. In Scheme 13 we look at $[2_a + 2_a]$ cycloadditions in more detail. For $Z_{\text{topo}} < 3$, there are, in principle, four possible modes for the double bond zipping, two of “zig-zag” (zz1 and zz2) and two of “armchair” (ac1 and ac2) type. In some cases where the rings possess certain symmetry, zz1 is equivalent to zz2, as is ac1 to ac2. We will use these notations in following discussions, so that every

Scheme 13. Four Modes of Double-Bond Zipping



time an ac or zz notation appears, that implies a certain sequence of $[2_a + 2_a]$ bond formations.

Similar to benzene \rightarrow degree-two polymer transformations, not only the $[2_a + 2_a]$ zipping but also $[4_a + 2_a]$ and $[4_a + 4_a]$ cycloadditions are able to transform a degree-two polymer to a degree-four polymer. However, as mentioned when discussing the collapse of degree-two polymers, careful examination shows that some $[2_a + 2_a]$, $[4_a + 2_a]$, and $[4_a + 4_a]$ cycloadditions lead to degree-four polymers that are dead ends toward degree-six polymers. These pathways are given in Figure S5 in the SI. Also, pathways that lead to four-membered rings are not considered. Of the 23 degree-four polymers (again not counting enantiomeric structures), only 7 are potentially productive for further polymerization to nanothreads, i.e., are not dead ends. These are the ones shown in Scheme 14.

It is noteworthy that there are five pathways that take the $-o_+ -$ polymer to five distinct degree-four polymers. One of these pathways, the $[4_s + 4_s]$ cycloaddition, which forms two bonds between two rings, leads to the $-B_+ - B_+ -$ polymer comprising *3uld* units. The remaining pathways all result in degree-four polymers composed of *2ud* units.

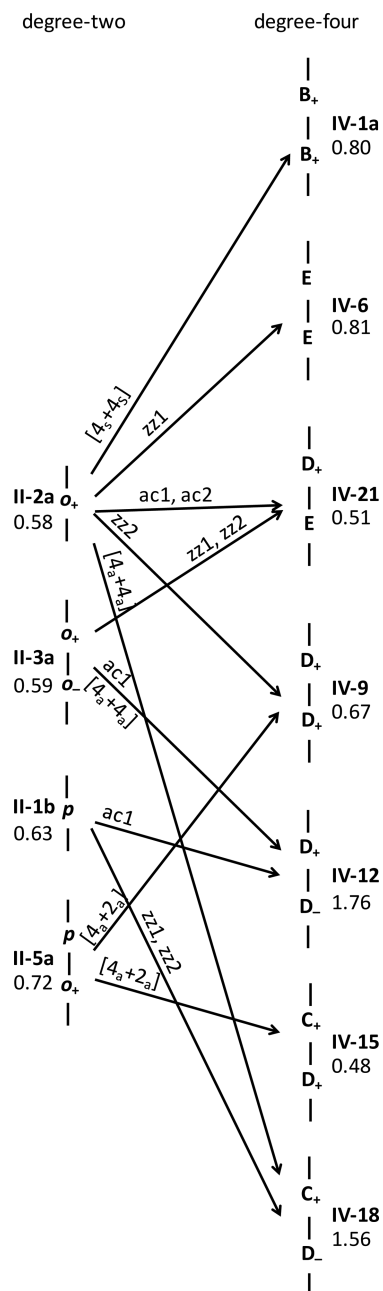
All the degree-four polymers in Scheme 14 and later in Schemes 15 and 16 are *syn* isomers, the ones that are able to further transform to a degree-six nanthread; any *anti* isomer is a dead end. For each of these degree-four *syn* isomers, we considered the four modes (zz1, zz2, ac1, ac2) of double bond zipping, as illustrated in Scheme 13. In certain cases, some of the four zipping modes give the same degree-six nanthread; some lead to four-membered ring structures. All these pathways and resultant degree-six nanthreads are shown in Scheme 15. We used the nomenclature introduced in our previous paper²⁰ to label different degree-six nanthreads.

It is interesting to note that all these degree-six nanthreads that can be formed via pathways in Scheme 15 are among the 15 lowest-energy nanthreads.

Following either pathway in Schemes 13–15, one needs three steps to convert benzene to a degree-six nanthread, each step increasing the degree of saturation by two. However, there is one pathway that increases the degree of saturation by four in one step, i.e., the $4 + 2$ polymerization of benzene to yield the $4 + 2$ polymer ($-E - E -$, IV-6), as shown in Scheme 2. We have combined the pathways in Schemes 13–15 as well as that increasing degree of saturation by four in one step in one diagram, which is shown in Scheme 16.

The world is not simple. If one needed any evidence of that, Scheme 16 provides it.

One can pick out pathways that go through intermediate polymers with relatively low energies. However, we must be careful to not assume that such pathways are favored over others. As we have not yet studied the barriers to these transformations, Scheme 16 is no more than it is, a list of smaller intermediate degree-two and degree-four polymers capable of going on in stepwise polymerization, and a list that also illustrates the topological relationships among benzene and

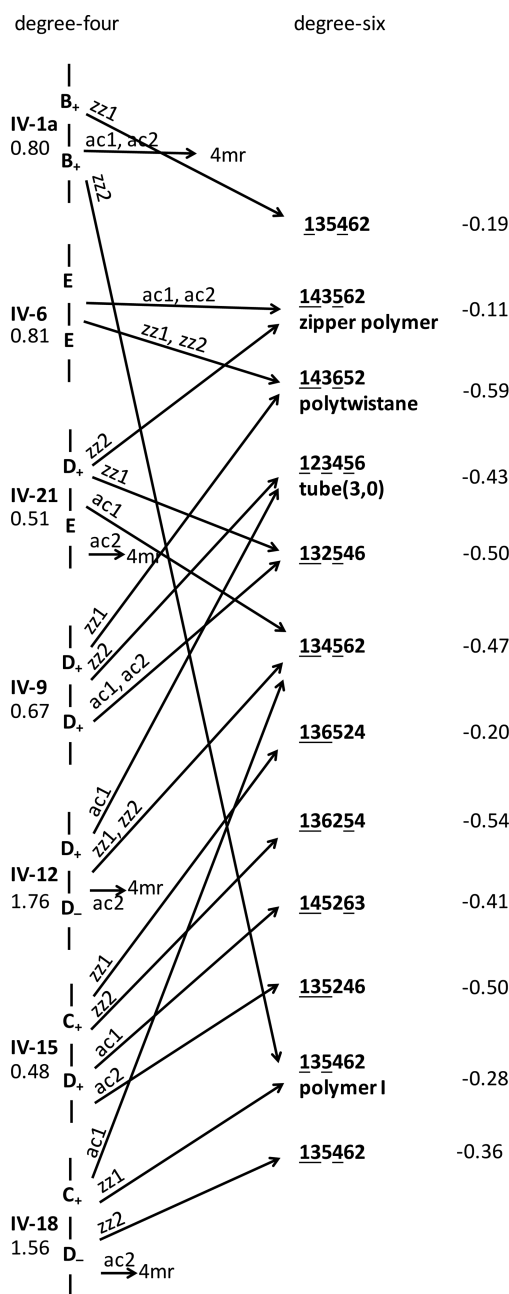
Scheme 14. Plausible Pathways from Degree-Two to Degree-Four Polymers That Can Further Transform to Degree-Six Nanotreads^a

^aThe name and energy, in units of eV/(CH)₆, of each polymer are given next to the sequence.

polymers of different degrees of saturation. This diagram could serve as a map and/or reference for further mechanistic studies, either experimental or theoretical. For example, if a radical initiator were to be effective in polymerization, the [4_s + 2_s] pathway among the five pathways starting from benzene would be excluded. Investigations of how benzene stacks react under pressure via these pathways are ongoing, and the results will be reported in due course.

SUMMARY AND CONCLUSIONS

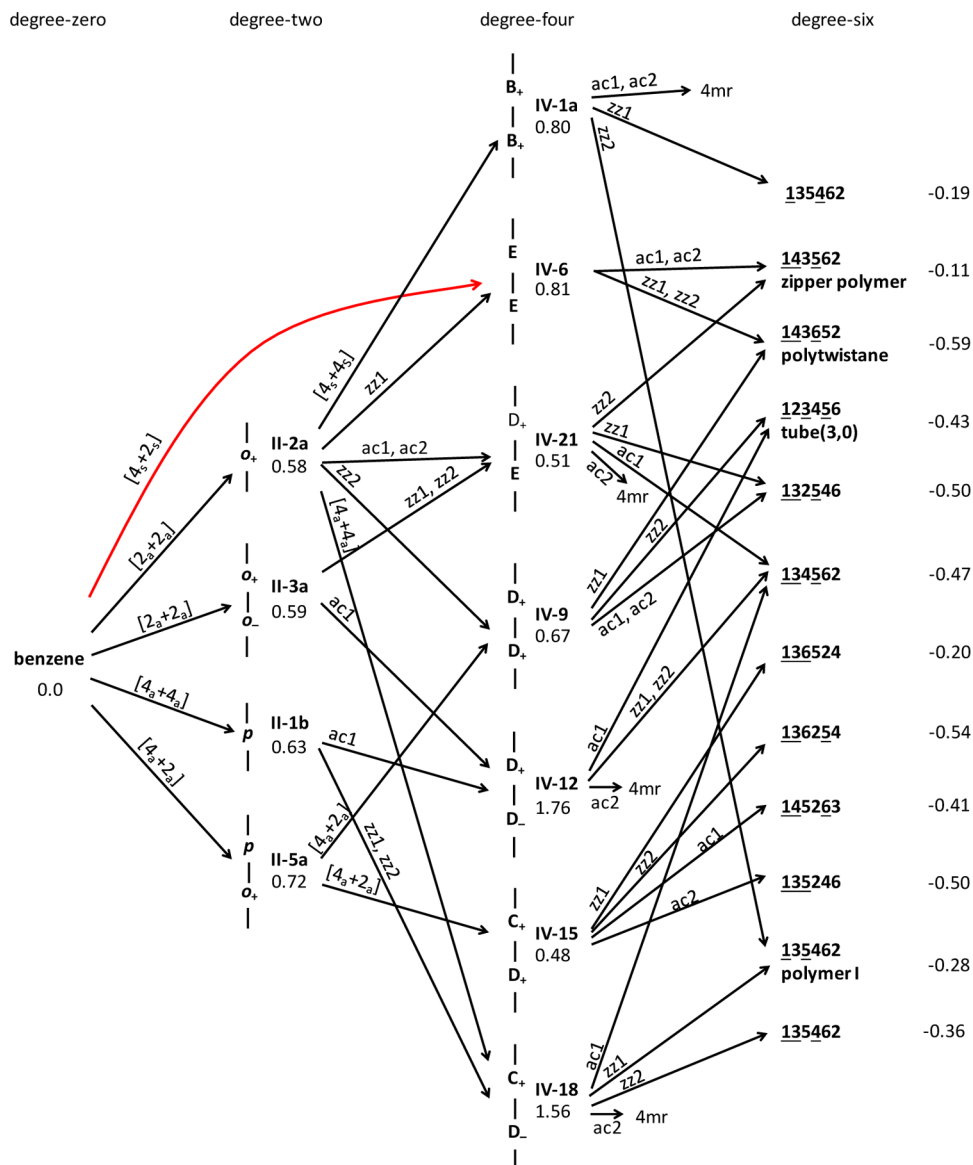
The polymerization under pressure of benzene to ordered fully saturated sp³ nanotreads, emerging as it does from high-

Scheme 15. Plausible Pathways from Degree-Four to Degree-Six^a

^aThe name and energy, in units of eV/(CH)₆, of each degree-four polymer are given next to the sequence. The nomenclature and energy for each degree-six nanotreads are also given.

pressure chemistry,⁴⁵ is but one beautiful example in an exciting research field, solid-state organic chemistry.⁴⁶ The formation of nanotreads is not simple. In the first of three theoretical approaches to the polymerization mechanism, we enumerate and categorize energetically the partially saturated 1-D (CH)₆ polymers. To facilitate the enumeration, the concept of degree of saturation—a count of how many sp³ carbons are in one (CH)₆ ring unit of the polymer—is introduced. It immediately suggests two types of intermediate polymers, with degrees of saturation two and four.

Structures of degree-two and four polymers are constructed from reasonable building blocks, with the following constraints:

Scheme 16. Plausible Pathways Connecting Benzene Stacks and Polymers of Different Degrees of Saturation^a

^aThe designation and energy, in units of $\text{eV}/(\text{CH})_6$, of each degree-two and degree-four polymer are given next to the sequence. The nomenclature and energy for each degree-six nanotubes are also provided.

(a) no radical structures, (b) no four-membered rings, (c) crystallographic unit cell $Z < 4$ for degree-two polymers, and (d) topological unit cell $Z_{\text{topo}} < 3$ for degree-four polymers. Eight topologically distinct degree-two polymers, each with one or more conformers arising from C–C bond rotations, were found. Some unstable conformers collapse without an energy barrier to degree-four polymers.

Twenty-three topologically distinct degree-four polymers were found. Among them, only the ones with the double bond in each ring approximately on the same side of the polymer chain, i.e., the *syn* isomers, are productive, in the sense that they can proceed to degree-six nanotubes; the others are dead ends.

The energetics we compute is of isolated linear polymers. With this assumption, there is an obvious caution. In real experimental systems there will be a role, perhaps a determinative one, for steric repulsion of neighboring stacks.

Interstack interactions will certainly affect relative energies, barriers to conformational transformations, and reaction paths.

Plausible reaction pathways comprising a variety of cyclo-additions that connect benzene, degree-two, four, and six polymers were examined. All degree-two polymers can be formed from benzene and all degree-four polymers from degree-two polymers. However, only 12 of the 15 lowest-energy degree-six nanotubes without four-membered rings can be formed from *syn* isomers of degree-four polymers; some with a four-membered ring can also be formed from *syn* isomers of degree-four polymers, while others require degree-four polymers with larger Z_{topo} and/or more complicated double-bond zipping.

With this database, the relative energies of a substantial number of $(\text{CH})_{6n}$ species, including benzene, benzene dimers, and 1D partially and fully saturated benzene polymers were compared, with 2D graphane, the most stable $(\text{CH})_m$ isomer as a reference. Except benzene, which is exceptionally stable due

to aromaticity, other (CH)_{6n} species follow the trend of decreasing energy with increasing degree of saturation.

The actual mechanism of nanothread formation from benzene under pressure is not yet clear. The overall kinetics of the degree zero-to-two, two-to-four, and four-to-six transformations, including whether they proceed by nucleation and growth or random polymerization, will depend on the relative reactivity of the benzene/benzene and benzene/polymer interfaces and may also be sensitive to structural relaxations induced by the action of high pressure upon the significant dimensional changes consequent to polymerization. The intermediate structural nature of the end-product—straddling the boundary between a rigid polymer and a 1-D solid-state crystal—suggests that elements from both polymer chemistry and solid-state crystal growth may come into play.

The plausible waypoints and pathways being delineated, we are, however, on the way to theoretical examination of the kinetic barriers to benzene stack polymerization. A helium compression chamber with benzene stacks in it will be used next to emulate the polymerization process under pressure.

■ COMPUTATIONAL METHODOLOGY

All calculations, except the molecular calculations on benzene dimer diradicals (see Figure S1 in the SI), are based on the plane-wave/pseudopotential approach using the VASP program,³³ employing the PBE exchange–correlation functional^{47,48} and the projector-augmented wave method.^{49,50} Dispersion correction was included by the zero damping DFT-D3 method of Grimme.⁵¹ The energy cutoff for the plane-wave basis was set to 500 eV. Each thread-like 1-D polymer was accommodated in a tetragonal unit cell (e.g., 10 Å × 10 Å × c Å), large enough to separate the thread far away from interacting with its replicas in adjacent unit cells. The axial lattice parameter c was scanned with step size 0.01 Å to obtain the optimal value. A 0.05 eV Gaussian smearing and a line of *k* points along the axial direction separated by <0.10 Å⁻¹ were used. The geometries of degree-six nanothreads were obtained from a previous work;²⁰ and single-point calculations were performed at these geometries to obtain energies that are comparable to other polymers and molecules. For each molecular species (benzene and benzene dimer), a cubic cell of 10 Å × 10 Å × 10 Å was used; only the gamma point was sampled. For the 3D benzene phase III structure, the tetrahedron method with Blöchl corrections⁵² and a 11 × 11 × 7 Monkhorst–Pack mesh⁵³ were employed. No pressure is applied in the calculations of 1-D polymers and molecular species; pressure of 1 atm or 20 GPa was applied in the geometry optimization of benzene phase III at that pressure. All graphics of polymer structures were generated by VESTA 3.⁵⁴

■ ASSOCIATED CONTENT

Supporting Information

This material is available free of charge via the Internet at <http://pub.acs.org>. The Supporting Information is available free of charge on the ACS Publications website at DOI: 10.1021/jacs.5b09053.

Figure S1–S5, energies and geometries of calculated structure (Table S1) (PDF)

Structures of degree-two and four polymers (ZIP, CIF)
Input file for 3D printer to print the benzene model (ZIP)

■ AUTHOR INFORMATION

Corresponding Author

*rh34@cornell.edu

Notes

The authors declare no competing financial interest.

■ ACKNOWLEDGMENTS

This work was supported by the Energy Frontier Research in Extreme Environments (EFree) Center, an Energy Frontier Research Center funded by the U.S. Department of Energy, Office of Science under award number DE-SC0001057.

■ REFERENCES

- (1) Bridgman, P. W. *Phys. Rev.* **1914**, *3*, 153.
- (2) Pruzan, Ph.; Chervin, J. C.; Thiéry, M. M.; Itié, J. P.; Besson, J. M.; Forgerit, J. P.; Revault, M. *J. Chem. Phys.* **1990**, *92*, 6910.
- (3) Cansell, F.; Fabre, D.; Petitet, J. P. *J. Chem. Phys.* **1993**, *99*, 7300.
- (4) Ciabini, L.; Santoro, M.; Bini, R.; Schettino, V. *J. Chem. Phys.* **2002**, *116*, 2928.
- (5) Jackson, B. R.; Trout, C. C.; Badding, J. V. *Chem. Mater.* **2003**, *15*, 1820.
- (6) Ciabini, L.; Gorelli, F. A.; Santoro, M.; Bini, R.; Schettino, V.; Mezouar, M. *Phys. Rev. B: Condens. Matter Mater. Phys.* **2005**, *72*, 094108.
- (7) Ciabini, L.; Santoro, M.; Gorelli, F. A.; Bini, R.; Schettino, V.; Mezouar, M. *Nat. Mater.* **2007**, *6*, 39.
- (8) Fitzgibbons, T.; Guthrie, M.; Xu, E.-S.; Crespi, V. H.; Davidowski, S. K.; Cody, G. D.; Alem, N.; Badding, J. V. *Nat. Mater.* **2015**, *14*, 43.
- (9) Stojkovic, D.; Zhang, P.; Crespi, V. H. *Phys. Rev. Lett.* **2001**, *87*, 125502.
- (10) Wen, X.-D.; Hoffmann, R.; Ashcroft, N. W. *J. Am. Chem. Soc.* **2011**, *133*, 9023.
- (11) Olbrich, M.; Mayer, P.; Trauner, D. *Org. Biomol. Chem.* **2014**, *12*, 108.
- (12) Barua, S. R.; Quanz, H.; Olbrich, M.; Schreiner, P. R.; Trauner, D.; Allen, W. D. *Chem. - Eur. J.* **2014**, *20*, 1638.
- (13) (a) Sluiter, M. H. F.; Kawazoe, Y. *Phys. Rev. B: Condens. Matter Mater. Phys.* **2003**, *68*, 085410. (b) Sofo, J. O.; Chaudhari, A. S.; Barber, G. D. *Phys. Rev. B: Condens. Matter Mater. Phys.* **2007**, *75*, 153401.
- (14) Wen, X.-D.; Hand, L.; Labet, V.; Yang, T.; Hoffmann, R.; Ashcroft, N. W.; Oganov, A. R.; Lyakhov, A. O. *Proc. Natl. Acad. Sci. U. S. A.* **2011**, *108*, 6833 and references therein.
- (15) Lian, C.-S.; Wang, X.-Q.; Wang, J.-T. *J. Chem. Phys.* **2013**, *138*, 024702.
- (16) He, C.; Sun, L. Z.; Zhang, C. X.; Zhong, J. J. *Phys.: Condens. Matter* **2013**, *25*, 205403.
- (17) Lian, C.-S.; Li, H.-D.; Wang, J.-T. *Sci. Rep.* **2015**, *5*, 7723.
- (18) Kondrin, M. V.; Brazhkin, V. V. *Phys. Chem. Chem. Phys.* **2015**, *17*, 17739.
- (19) Maryasin, B.; Olbrich, M.; Trauner, D.; Ochsenfeld, C. *J. Chem. Theory Comput.* **2015**, *11*, 1020.
- (20) Xu, E.-S.; Lammert, P. E.; Crespi, V. H. *Nano Lett.* **2015**, *15*, 5124.
- (21) We note in the context the fascinating studies of ethylene, acetylene and CO polymerization in zeolite matrixes: (a) Santoro, M.; Gorelli, F. A.; Bini, R.; Haines, J.; van der Lee, A. *Nat. Commun.* **2013**, *4*, 1557. (b) Scelta, D.; Ceppatelli, M.; Santoro, M.; Bini, R.; Gorelli, F. A.; Perucchi, A.; Mezouar, M.; van der Lee, A.; Haines, J. *Chem. Mater.* **2014**, *26*, 2249. (c) Santoro, M.; Dziubek, K.; Scelta, D.; Ceppatelli, M.; Gorelli, F. A.; Bini, R.; Thibaud, J.-M.; Di Renzo, F.; Cambon, O.; Rouquette, J.; Hermet, P.; van der Lee, A.; Haines, J. *Chem. Mater.* **2015**, *27*, 6486.
- (22) Thiéry, M. M.; Léger, J. M. *J. Chem. Phys.* **1988**, *89*, 4255.
- (23) Benzene phase III', which was suggested by Thiéry and Léger²² to also exist in this pressure range, has not been observed in a later work by Ciabini et al.^{6,7}
- (24) While most of the crystal is stable in the pressure range, a tiny fraction of benzene (~0.01%) begin to oligomerize at about 13 GPa, see Shinozake, A.; Mimura, K.; Kagi, H.; Komatsu, K.; Noguch, N.; Gotou, H. *J. Chem. Phys.* **2014**, *141*, 084306.
- (25) The 3D model was made from computed geometries of the structure by following the procedure described in the following paper:

“How to print a crystal structure model in 3D”, *CrystEngComm*, **2014**, *16*, 5488. We provide in the [Supporting Information](#) the file needed for 3D printing the model shown in [Figure 1](#). Interested readers can print their own benzene models with our file.

(26) The Bini group proposed that at high pressure an excited state ($^1B_{2u}$) of benzene forms, which initiates the polymerization to amorphous hydrocarbon, see ref 4. The same group also found that photoinduced polymerization of benzene occurs at a lower pressure, in which the same excited state ($^1B_{2u}$) was proposed as the initiator. See (a) Ciabini, L.; Santoro, M.; Bini, R.; Schettino, V. *Phys. Rev. Lett.* **2002**, *88*, 085505. (b) Citroni, M.; Bini, R.; Foggi, P.; Schettino, V. *Proc. Natl. Acad. Sci. U. S. A.* **2008**, *105*, 7658.

(27) Woodward, R. B.; Hoffmann, R. *Angew. Chem., Int. Ed. Engl.* **2003**, *8*, 781.

(28) Olbrich, M.; Mayer, P.; Trauner, D. *J. Org. Chem.* **2015**, *80*, 2042.

(29) 4 + 2 oligomers (but not the polymer) have been synthesized by Grimme et al. (a) Grimme, W.; Reinhardt, G. *Angew. Chem., Int. Ed. Engl.* **1983**, *22*, 617. (b) Grimme, W.; Gossel, J.; Lex, J. *Angew. Chem., Int. Ed.* **1998**, *37*, 473.

(30) Jenkins, A. D. *Pure Appl. Chem.* **1981**, *53*, 733.

(31) Dennington, R.; Keith, T.; Millam, J. *GaussView*, version 5; Semichem Inc.: Shawnee Mission, KS, 2009.

(32) Schaftenaar, G.; Noordik, J. H. *J. Comput.-Aided Mol. Des.* **2000**, *14*, 123.

(33) Kresse, G.; Hafner, J. *Phys. Rev. B: Condens. Matter Mater. Phys.* **1993**, *47*, 558.

(34) The heats of formation ($\Delta_f H^\circ_{\text{gas}}$) of 1,3- and 1,4-cyclohexadiene are, respectively, 104.58 ± 0.63 and 104.75 ± 0.59 kJ/mol, see Steele, W. V.; Chirico, R. D.; Nguyen, A.; Hossenlopp, I. A.; Smith, N. K. *AIChE Symp. Ser.* **1989**, *85*, 140.

(35) Houk, K. N.; Lin, Y. T.; Brown, F. K. *J. Am. Chem. Soc.* **1986**, *108*, 554.

(36) Dewar, M. J. S.; Olivella, S.; Stewart, J. J. P. *J. Am. Chem. Soc.* **1986**, *108*, 5771.

(37) The *syn/anti* notations are originally used to describe whether the two substituents are added to the same side or opposite sides of an unsaturated bond in an addition reaction. In time it was extended to name isomers, as in the 2 + 2 benzene molecular dimers.

(38) Stewart, J. J. P. *J. Comput. Chem.* **1989**, *10*, 209.

(39) B3LYP is a combination of Becke's 3-parameter hybrid exchange functional (Becke, A. D. *J. Chem. Phys.* **1993**, *98*, 5648) with the electron correlation functional of Lee, Yang, and Parr (Lee, C.; Yang, W.; Parr, R. G. *Phys. Rev. B* **1988**, *37*, 785).

(40) Frisch, M. J.; Trucks, G. W.; Schlegel, H. B.; Scuseria, G. E.; Robb, M. A.; Cheeseman, J. R.; Scalmani, G.; Barone, V.; Mennucci, B.; Petersson, G. A.; Nakatsuji, H.; Caricato, M.; Li, X.; Hratchian, H. P.; Izmaylov, A. F.; Bloino, J.; Zheng, G.; Sonnenberg, J. L.; Hada, M.; Ehara, M.; Toyota, K.; Fukuda, R.; Hasegawa, J.; Ishida, M.; Nakajima, T.; Honda, Y.; Kitao, O.; Nakai, H.; Vreven, T.; Montgomery, J. A., Jr.; Peralta, J. E.; Ogliaro, F.; Bearpark, M.; Heyd, J. J.; Brothers, E.; Kudin, K. N.; Staroverov, V. N.; Kobayashi, R.; Normand, J.; Raghavachari, K.; Rendell, A.; Burant, J. C.; Iyengar, S. S.; Tomasi, J.; Cossi, M.; Rega, N.; Millam, J. M.; Klene, M.; Knox, J. E.; Cross, J. B.; Bakken, V.; Adamo, C.; Jaramillo, J.; Gomperts, R.; Stratmann, R. E.; Yazyev, O.; Austin, A. J.; Cammi, R.; Pomelli, C.; Ochterski, J. W.; Martin, R. L.; Morokuma, K.; Zakrzewski, V. G.; Voth, G. A.; Salvador, P.; Dannenberg, J. J.; Dapprich, S.; Daniels, A. D.; Farkas, Ö.; Foresman, J. B.; Ortiz, J. V.; Cioslowski, J.; Fox, D. J. *Gaussian 09*, Revision D.01, Gaussian, Inc., Wallingford CT, 2009.

(41) However, these dead-end polymers in the solid state could cross-link with adjacent polymers.

(42) (a) Sanderson, R. T. *Polar Covalence*; Academic Press: New York, 1983. (b) Sanderson, R. T. *Chemical Bonds and Bond Energy*; Academic Press: New York, 1976.

(43) The heats of formation ($\Delta_f H^\circ_{\text{gas}}$) of ethylene and cyclohexane are, respectively, 52.47 and -123.1 ± 0.79 kJ/mol, see (a) Chase, M. W., Jr. *J. Phys. Chem. Ref. Data, Monograph* **1998**, *9*, 1. (b) Prosen, E. J.; Johnson, W. H.; Rossini, F. D. *J. Res. NBS* **1946**, *37*, 51.

(44) Schleyer, P. v. R. *Chem. Rev.* **2001**, *101*, 1115 and following reviews in this issue.

(45) (a) Badding, J. V. *Annu. Rev. Mater. Sci.* **1998**, *28*, 631. (b) Schettino, V.; Bini, R.; Ceppatelli, M.; Ciabini, L.; Citroni, M. *Advances in Chemical Physics* **2005**, *131*, 105. (c) McMillan, P. F. *Chem. Soc. Rev.* **2006**, *35*, 855.

(46) (a) Toda, F. *Acc. Chem. Res.* **1995**, *28*, 480. (b) *Organic Solid State Reactions, Topics in Current Chemistry*; Toda, F., Ed.; Springer-Verlag: Berlin, 2005; Vol 254.

(47) Perdew, J. P.; Burke, K.; Ernzerhof, M. *Phys. Rev. Lett.* **1996**, *77*, 3865.

(48) Perdew, J. P.; Burke, K.; Ernzerhof, M. *Phys. Rev. Lett.* **1997**, *78*, 1396.

(49) Blöchl, P. E. *Phys. Rev. B: Condens. Matter Mater. Phys.* **1994**, *50*, 17953.

(50) Kresse, G.; Joubert, D. *Phys. Rev. B: Condens. Matter Mater. Phys.* **1999**, *59*, 1758.

(51) Grimme, S.; Antony, J.; Ehrlich, S.; Krieg, S. *J. Chem. Phys.* **2010**, *132*, 154104.

(52) Blöchl, P. E.; Jepsen, O.; Anderson, O. K. *Phys. Rev. B: Condens. Matter Mater. Phys.* **1994**, *49*, 16223.

(53) Monkhorst, H. J.; Pack, J. D. *Phys. Rev. B* **1976**, *13*, 5188.

(54) Momma, K.; Izumi, F. *J. Appl. Crystallogr.* **2011**, *44*, 1272.